Microfluid Nanofluid (2015) 18:111–120
DOI 10.1007/s10404-014-1422-y

RESEARCH PAPER

Nanoparticle-tuned spreading behavior of nanofluid droplets on the solid substrate

YingQi Li · FengChao Wang · He Liu · HengAn Wu

Received: 22 December 2013 / Accepted: 7 May 2014 / Published online: 17 May 2014

Abstract Nanofluids, which are the term for suspensions of nanometer-sized structures, have recently been extensively used in a rapid increasing number of applications. In this work, spreading behaviors of water-based nanofluid droplets were investigated via molecular dynamics simulation. Influencing factors such as nanoparticle volume fraction and surface wettability were discussed in details on the atomic scale. Our simulation results demonstrated that the dynamics spreading of nanofluids can be effectively regulated by adjusting these factors. Based on the scaling law $R(t) \propto t^{1/n}$, we proposed a competitive mechanism analysis among surface tension, viscous force and disjoining pressure, which describes the power relationship between contact radius R and spreading time t. These findings indicate that the nanoparticle-tuned spreading behavior of nanofluid droplets can be extensively used for diverse applications.

1 Introduction

It has been a long history of the use of nanosuspension and nanoparticles, like pharmacy (Chen and Bodmeier 1990) and drug delivery (Oppenheim 1981). In 1995, Choi et al. first introduced the word "nanofluid" to describe this engineering medium which was produced by adding nanostructures, such as nanoparticles, nanowires to base fluid like water, oil and alcohols (Choi and Eastman 1995; Lee et al. 1999). Enhancements in various properties of nanofluids such as thermal conductivity (Chon et al. 2005; Hong et al. 2005; Baby and Ramaprabhua 2010), electrical conductivity (Baby and Ramaprabhua 2010; Minea and Luciu 2012; Ganguly et al. 2009) and viscosity (Prasher et al. 2006; Kole and Dey 2010) have been extensively studied.

In recent years, experiments reported that the presence of nanoparticles also changes the wetting behaviors of nanofluids compared to that of base liquid (Wasan and Nikolov 2003). Consequently, understanding and controlling of the dynamic spreading of nanofluid droplet have gained significant attention. Liu et al. (2006) proposed an optofluidic control method using suspended photothermal nanoparticles near the liquid–air interface, which can drive and guide the liquid flow in microfluidic channels. In previous research, influencing factors like nanoparticle volume fraction, nanoparticle surface properties, particle size and particle morphology were concerned. Vafaei et al. (2006) observed that the equilibrium contact angle of droplet laden with nanoparticles on both hydrophilic and hydrophobic substrates is sensitive to nanoparticle concentration, as well as nanoparticle size. Disjoining pressure acting in the vicinity of triple-phase contact line is considered to be a vital factor for the enhanced spreading of nanofluid on a solid surface (Wasan and Nikolov 1999, 2003; Trokhymchuk et al. 2001; Ritos et al. 2013).

There is considerable interest in the wetting and dewetting phenomena of liquid droplet in various length scales (Kondiparty et al. 2011; Nieminen et al. 1992; De Ruijter et al. 1999; Song et al. 2013; Alava and Dube 2012;

Y. Li · F. Wang (✉) · H. Liu · H. Wu (✉)
CAS Key Laboratory of Materials Behavior and Design of Materials, Department of Modern Mechanics, University of Science and Technology of China, Hefei 230027, Anhui, China
e-mail: wangfc@ustc.edu.cn

H. Wu
e-mail: wuha@ustc.edu.cn

H. Liu
PetroChina Research Institute of Petroleum Exploration and Development, Beijing 100083, China

Adao et al. 1999). It has long been known that Tanner's spreading law indicates a power relationship between the contact radius of a liquid droplet and the spreading time (Tanner 1979). Governing equations of droplet spreading are deduced from the Navier–Stokes and continuity equations (Oron et al. 1997; Zhao 2012). Heine et al. (2005) then found that the spreading of precursor film predicts a droplet-size dependence in both non-wetting and wetting cases, which results from the higher bulk spreading rate of the larger droplets pushes the precursor foot outward adding to the driving force of the surface interaction. For nanodroplet, precursor film propagates faster than the bulk droplet (Yuan and Zhao 2010).

Although these efforts have been devoted, spreading mechanisms of nanofluid droplet laden with well-distributed nanoparticles are still not clear at present. Previous research shows that nanoparticles regulate surface tension (Pilkington and Briscoe 2012) and viscous force (Prasher et al. 2006; Kole and Dey 2010) of nanofluids. The underlying mechanism about how these forces evolve and dominate the spreading process has not been well understood. Meanwhile, whether the well-accepted theories of pure water droplet, for instance, the scaling law mentioned above, could be applied to describe the nanofluid droplet spreading remains to be discussed.

Despite the above-mentioned experimental and theoretical studies in the past decade, we found that there is lack of molecular details and deeper understanding on the nanofluid spreading. In this work, we intend to give a detailed representation of how factors such as nanoparticle volume fraction and surface wettability regulate the nanofluid droplet spreading process, focusing on both the equilibrium state and dynamic evolution of the contact radius. First, we successfully set up molecular modeling of the nanofluids and carried out MD simulations on nanofluid spreading. Then, we monitored how contact radius R varied with spreading time t and validated that the $R(t)$ relationship of nanofluid droplet can be described by the scaling law. After that, we applied the scaling law, which is based on lubrication approximation theory to explain the nanofluid droplet spreading behavior. In this way, we interpreted the nanoparticle-tuned spreading behavior of nanofluids. Finally, a competitive mechanism among surface tension, viscous force and disjoining pressure was proposed. In addition, further quantitative analysis demonstrates that the inherent viscous force of nanofluids dominates in the competitive mechanism. This work provides new application ideas of nanofluid in many industry practices like enhanced oil recovery (Wang and Wu 2013).

2 Model and simulation details

Our MD simulations were carried out using LAMMPS package (Plimpton 1995). To explore the spreading behavior of the water-based nanofluid droplet on a solid substrate, we built two-dimensional cylindrical models shown in Fig. 1. The simulation system contains a water-based nanofluid droplet laden with well-distributed sphere nanoparticles and a solid substrate.

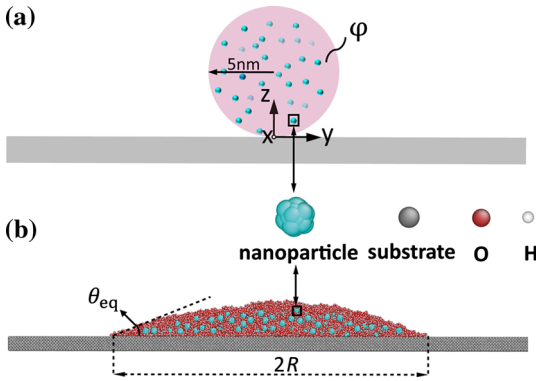

Fig. 1 Schematic plots of the simulation system. **a** Diagrammatic drawing of the initial configure of the simulation system: a cylinder nanofluid droplet laden with well-dispersed nanoparticles is placed on the solid substrate. φ denotes the nanoparticle volume fraction. **b** MD snapshot of the nanofluid droplet spreading equilibrium state ($\varphi = 3$ %). θ_{eq} and R indicate the equilibrium contact angle and the contact radius, respectively

The substrate used in our study is constructed based on the face-centered cubic crystal lattice structure, with a total number of 39,600 atoms. The lattice constant is 3.0 Å. During the simulations, the substrate was fixed so that we need not calculate the interactions between their own atoms, which significantly reduced the simulation time. Each nanoparticle contains 33 atoms, which were placed on a cubic lattice within a sphere with a diameter of 0.5 nm. The lattice spacing is 0.2 nm. During the spreading process, each nanoparticle was treated to be an independent rigid body, which means that each nanoparticle moves and rotates as a single entity. We also studied nanofluid droplets laden with larger nanoparticles of diameter about 1.0 nm. And each larger nanoparticle contains 257 atoms. In the present work, the nanoparticles are well dispersed in water when we set up the initial configuration. Moreover, the interactions between nanoparticles [controlled by Lennard-Jones (LJ) parameters] are set to be relatively small, which makes it difficult for nanoparticles to agglomerate (Lin et al. 2011). The agglomeration has not been observed during all our simulations.

In the MD simulations, we prefer to study the surface properties effect of the substrate and nanoparticles in a wider range, rather than to demonstrate a specific solid material. If a certain atom type is specified, its LJ interaction with liquid is always a fixed value, it is not appropriate to adjust the LJ parameters to study the wettability effects. For this reason, atoms of substrate and

nanoparticles are all not specified in this work. Since we concentrated on the spreading process of nanofluid, the wettability property of substrate can be adjusted by changing the LJ interaction parameters between liquid and nanoparticle/substrate in an appropriate range.

We conducted MD simulations to study the contact line migration of nanofluid droplet by altering interaction energies between water–substrate, water–nanoparticle and nanoparticle–substrate. Parameters of oxygen atoms and hydrogen atoms refer to the SPC/E water model (Berendsen et al. 1987). Characteristic energy values of oxygen ε_O and hydrogen ε_H are severally to be 0.1554 and 0 kcal/mol. Besides, hydrogen and oxygen atoms are electrically charged +0.4238e and −0.8476e, respectively. Both nanoparticles and the solid atoms in the substrate have no charge. A standard 12-6 LJ potential is used to describe the van der Waals interactions between solid and liquid atoms. Coulomb interactions among water molecules are calculated through Eq. (2) to account for electrostatic effects. These potential functions are given by

$$U_{\mathrm{LJ}} = 4\varepsilon_{ij}\left[\left(\frac{r_{ij}^{\min}}{r_{ij}}\right)^{12} - \left(\frac{r_{ij}^{\min}}{r_{ij}}\right)^{6}\right], \tag{1}$$

$$U_{\mathrm{coulomb}} = \frac{q_i q_j}{4\pi\varepsilon_0 r_{ij}}, \tag{2}$$

in which r_{ij} is the distance between atoms i and j. In Eq. (1), ε_{ij} is the characteristic energy and $r_{\mathrm{ij}}^{\min}$ is the distance at which the potential reaches zero. In Eq. (2), q_i and q_j are the charges on the 2 atoms, ε_0 is the vacuum permittivity. For van der Waals interactions between different species, LJ parameters obey the mixing rules represented in Eq. (3)

$$\varepsilon_{ij} = \sqrt{\varepsilon_i \cdot \varepsilon_j},\ r_{ij}^{\min} = \left(r_i^{\min} + r_j^{\min}\right)\Big/2. \tag{3}$$

Surface wettability of the substrate and nanoparticles was acquired via changing the characteristic energy of the solid atom ε_s or that of nanoparticle atom ε_n. The parameters of each model will be presented later in the next section.

MD simulations were performed in NVT ensemble. Cutoff values for LJ interactions and Coulombic interactions were set to be 10 and 12 Å, respectively. The long-range electrostatic interactions were computed using the PPPM algorithm, with a convergence parameter of 10^{-4}. The cylinder nanofluid droplet model was placed in a simulation box of 33 × 600 × 220 Å. X direction is the axial direction of the cylinder droplet (as Fig. 1a illustrates), and the length along X is rather small compared with that along Y. Periodic boundary condition is applied to X and Y directions so that this model is quasi-two-dimensional, whereas free boundary is applied to Z direction. The droplet keeps constant thickness along X direction during the simulation process. Velocity verlet algorithm with a time step 1 fs was used to integrate Newton's motion equations. The temperature of nanofluid was kept constant at 298 K by employing a Nosé–Hoover thermostat with a temperature damping coefficient of 0.1 ps.

Table 1 Composition of different nanoparticle volume fraction models

Model number	Nanoparticle volume fraction φ (%)	Number of water molecules N_w	Number of nanoparticles N_n	Viscosity of nanofluid μ (10^{-3}Pa s)
1	0	7,853	0	0.927
2	1	7,774	70	1.169
3	3	7,617	211	2.045
4	5	7,460	352	4.376

We initially placed the nanofluid droplet separately above the substrate with a 3 Å distance. After that, the interactions between the liquid and the solid start to develop and the nanofluid droplet start to spread. This is a conventional method in MD simulations to study the spreading dynamics (Heine et al. 2005). Then after an energy minimization process, we conducted MD simulations for 2×10^6 time steps (2 ns) to make sure that the droplets reached the equilibrium state.

To study the effect of nanoparticle volume fraction on nanofluid droplet spreading, models with different nanoparticle volume fractions were set up. The water molecule number N_w and nanoparticle number N_n in each model are listed in Table 1.

We fixed the characteristic interaction energy between different atom types; that is, characteristic interaction energy between solid surface atoms and oxygen atoms is $\varepsilon_{so} = 0.25$ kcal/mol; nanoparticle–nanoparticle $\varepsilon_{nn} = 0.01$ kcal/mol; nanoparticle–solid surface $\varepsilon_{ns} = 0.01$ kcal/mol. In study of nanoparticle volume fraction effects, nanoparticle–oxygen is set to be $\varepsilon_{no} = 0.2$ kcal/mol.

Another important factor that may potentially affect nanofluid droplet spreading is the surface properties of the nanoparticles, mainly means the surface wettability. Here, we select $\varphi = 5$ % nanofluid droplet model to study this factor. The surface wettability of nanoparticles is related to the characteristic interaction energy between nanoparticles and oxygen atoms, ε_{no}, and is adjusted by changing the value of ε_{no}. Considering that in model 4 $\varepsilon_{no} = 0.2$ kcal/mol, we employed another three values, that is $\varepsilon_{no} = 0.1$ (model 5), 0.15 (model 6) and 0.3 (model 7) kcal/mol, and the rest interaction parameters are the same as above.

3 Results and discussion

3.1 Nanoparticle concentration effect on nanofluid droplet spreading

3.1.1 Equilibrium state

Figure 2b provides the final spreading shape at 2 ns, and equilibrium contact angles of nanofluid droplets contain different amount of nanoparticles. We first note that water droplet reached an equilibrium state with a small but finite contact angle about 9°, which is in agreement of previous results (de Gennes 1985). It should be noted that in the present study, it is not easy and accuracy to distinguish the precursor film and the bulk droplet. So we calculated the contact angles without removing the precursor film. Considering that nanoparticles distribute randomly in the nanofluid during simulation, and even at equilibrium state, the final spreading snapshots of nanofluid droplet shown would have small perturbation and thus are unsymmetric. We averaged density contours around equilibrium state and fetched the outline of the density contours as averaged final spreading shape, shown in Fig. 2a. It is obvious that results in Fig. 2a have better symmetry after averaging.

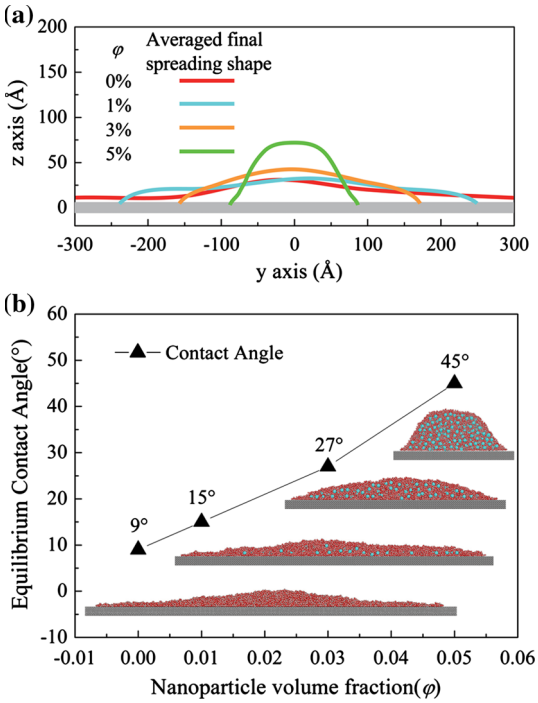

Fig. 2 Spreading result of nanofluid droplet with different nanoparticle concentration. **a** Comparison of averaged droplet profiles around the final equilibrium state, which intuitively reveals the nanoparticle-tuned spreading behavior of nanofluid droplet. **b** Final MD snapshots of each model and their equilibrium contact angles θ_{eq}, respectively

Nanofluid droplets exhibit obvious difference at final equilibrium state even with small nanoparticle volume fraction, say $\varphi = 1$ %. First, a precursor film consisting of several layers of atoms appears around the bulk droplet. However, there is no noticeable precursor film around the nanofluid droplets. It is widely believed that the motion of precursor film is driven by a gradient of disjoining pressure (de Gennes 1985; Yuan and Zhao 2010).

Then, we note there is a clear trend that the equilibrium contact angle of nanofluid increases with increasing nanoparticle volume fraction. In another words, the existence of nanoparticles tends to inhibit nanofluid droplet from spreading. And as φ varies from 1 to 5 %, this spreading-inhibition effect become more significant, and the equilibrium contact angle increases dramatically from 9° to about 45°.

As we know that $W_c = 2\gamma_{lv}$ is the work of cohesion of the liquid droplet. $W_a = \gamma_{lv} + \gamma_{sv} - \gamma_{sl}$ is the work of adhesion for the interface between the liquid and the substrate. And the spreading coefficient S, defined as $S = W_a - W_c = \gamma_{sv} - (\gamma_{sl} + \gamma_{lv})$, is generally used to describe the spreading of liquid on a solid surface (Harkins and Feldman 1922). Where γ_{lv}, γ_{sv}, γ_{sl} are the surface tension between liquid–vapor, solid–vapor and solid–liquid, respectively. Spreading occurs when adhesion between liquid and solid is greater than the inner cohesion of liquid. That means $S \geq 0$ corresponds to complete wetting and $S < 0$ to partial wetting (Harkins and Feldman 1922). In terms of our results, the existence of nanoparticles enhanced the internal cohesion of the nanofluid droplet due to their interactions with water molecules, including intermolecular attraction and friction, which makes the nanofluid droplet more difficult to spread. The almost completely spreading of water droplet (model 1) indicates a $S \geq 0$ state. As nanoparticles volume fraction increased, the nanofluid changed from an almost complete wetting to partial wetting.

The enhancement of cohesion in nanofluid also indicates the increase in nanofluid surface tension, γ_{lv}. This confirms with the previous study (Pilkington and Briscoe 2012). It also should be note that since nanoparticles would regulate the surface tension of nanofluid. So the nanofluid surface tension γ_{lv} here is an effective surface tension related to the nanoparticles volume fraction and surface wettability. Young's equation: $\cos\theta_{eq} = (\gamma_{sv} - \gamma_{sl})/\gamma_{lv}$ describes the equilibrium force balance at the contact line region of droplet (de Gennes 1985). Increase in γ_{lv} gives rise to increase in equilibrium contact angle θ_{eq}. Our simulation result that equilibrium contact angle increases with increasing nanoparticle volume fraction supports this point.

3.1.2 Variation of contact radius during spreading

Then we employed the contact radius R as an index to quantitatively describe the spreading rate of nanofluid

droplet on the solid surface. These data points were obtained by calculating the contact diameter every 0.05 ns, and contact radius R is half of the contact diameter.

In Fig. 3a, the contact radius data from all models are in good consistence with a power exponential function: $R(t) = at^{1/n}$, and the fitting value of coefficients a and n for each model is presented in Table 2. These results indicate that the well-known power law, $R(t) \propto at^{1/n}$, can be applied to describe the spreading behavior of nanofluid droplet laden with nanoparticles, which agrees with experimental result (Han and Kim 2012).

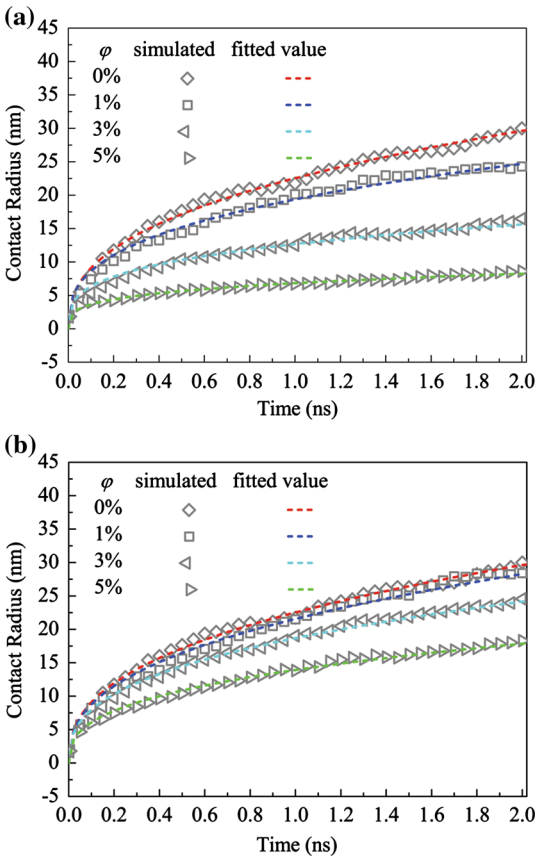

Fig. 3 **a** Statistical analysis of the variation of contact radius R as a function of the spreading time t. The *rhombus*, *cubic*, *left-triangle* and *right-triangle symbols,* respectively, refer to the measured contact radius values of nanofluid droplets with $\varphi = 0$, 1, 3 and 5 %. The *dash lines* in the graph are numerical fitting curves, with a fitting function described by $R(t) = at^{1/n}$. **b** The $R(t)$ relationship of nanofluid droplets contains larger nanoparticles ($d \approx 1.0$ nm)

Table 2 Fitting function coefficients of different fraction models

Model number	Nanoparticle volume fraction φ (%)	Fitting coefficient a	Fitting coefficient n
1	0	22.54	2.54
2	1	19.37	2.86
3	3	12.68	3.30
4	5	6.82	3.67

As shown in Fig. 3a, the nanofluid and water droplets present a similar spreading behavior: The droplet expands quickly at an early time, then spreads smoothly and finally reaches a relatively equilibrium state. The period of quick expanding shows a remarkable dependence on the nanoparticle volume fraction. For relatively higher nanoparticle concentration models $\varphi = 3$ and 5 %, the relatively quick expanding of contact radius appears only in the first 0.2 ns. While for water droplet and the nanofluid droplet with $\varphi = 1$ %, this quick expanding state lasts for a longer time, about 0.5 ns.

In terms of the values of scaling law, Tanner's law shows a 1/7 exponent. Yuan and Zhao (2010) indicate that precursor film of nanodroplet propagates faster than the bulk droplet. The reference also mentioned that without considering the precursor film, when equilibrium contact angle $\theta_{eq} \to 0$, $R(t) \sim t^{1/5}$ was obtained. As Fig. 1 illustrates, we observed the bulk droplet and precursor film to calculate values of R. So it is credible that when interactions between solid and liquid are large, the length of precursor film is remarkable; thus, exponents in our results are larger than 1/7 in Tanner's law. These results show that when discussing the fast propagation of the precursor film, the contribution of the disjoining pressure to the driving work of the spreading droplet should be taken into consideration (Yuan and Zhao 2010).

So it is obvious that as φ varies from 0 to 5 %, the contact radius reduced in both true length and growth rate. At final equilibrium state, the contact radius of water droplet reaches almost 3 nm, but for the $\varphi = 5$ % nanofluid droplet, contact radius at equilibrium state is only about 0.6 nm. This significant difference demonstrates the spreading-inhibition effect mentioned above. For further support, we calculated a supplementary model with $\varphi = 7$ %. As expected, the equilibrium contact angle turned out to be more than 130° and the nanofluid droplet almost does not spread.

It is widely believed that contact line motion can reflect the spreading of droplet (Han and Kim 2012), and the derivative of $R(t)$ exactly reflects the motion speed of the contact line. In Fig. 3a, increasing nanoparticle volume fraction will increase the nanofluid viscosity, thus result in reduction of the contact line motion speed of nanofluid droplets. This result is credible according to the above analysis of spreading coefficient S. Several mechanisms have been proposed to interpret similar phenomena, among which are nanoparticle accumulation and layering in the vicinity of triple-phase contact line as well as the pinning effect they caused (Wasan and Nikolov 2003; Trokhymchuk et al. 2001; Ritos et al. 2013).

Nanofluid droplet contains larger nanoparticles ($d \approx 1.0$ nm), with $\varphi = 1, 3, 5$ % were also calculated and their $R(t)$ curves are also obtained, shown as Fig. 3b. We note that the larger nanoparticle models showed a similar trend as the models we studied in Fig. 3a. This demonstrates that the trends we derived in Fig. 3a are credible. However, the inhibiting effect of larger nanoparticles on nanofluid spreading seems weaker than that of models in Fig. 3a. This is because at the same volume fraction, the larger the nanoparticle size is, the fewer the nanoparticles will be. Thus, the number of surface atoms that directly react with the water molecules will decrease.

3.2 Effect of surface wettability of nanoparticles

In Fig. 4, for all these models, the contact radius of nanofluid droplet changes corresponding to the spreading scaling law: $R(t) = at^{1/n}$, and the fitting coefficients are listed in Table 3.

Several trends can be concluded from Fig. 4. First, our simulation results show that the spreading behaviors of nanofluid droplets are sensitive to the surface properties of nanoparticles. In addition, when the nanoparticles are sufficiently hydrophilic, such as when $\varepsilon_{no} = 0.30$ kcal/mol, the nanofluid droplet spreads slightly, with an equilibrium contact angle of about 90°. If we continually increase the nanoparticle–water interactions to $\varepsilon_{no} = 0.5$ kcal/mol, the equilibrium contact angle exceeds 120°. This indicates that the spreading coefficient S gradually tends to be negative when interaction between nanoparticles and water molecules increases, which in turn demonstrates that the increase of interaction between nanoparticles and water molecules enhances the internal cohesive of nanofluid. Therefore, it is feasible to control the dynamic behaviors of nanofluid droplet through changing the surface properties of nanoparticles.

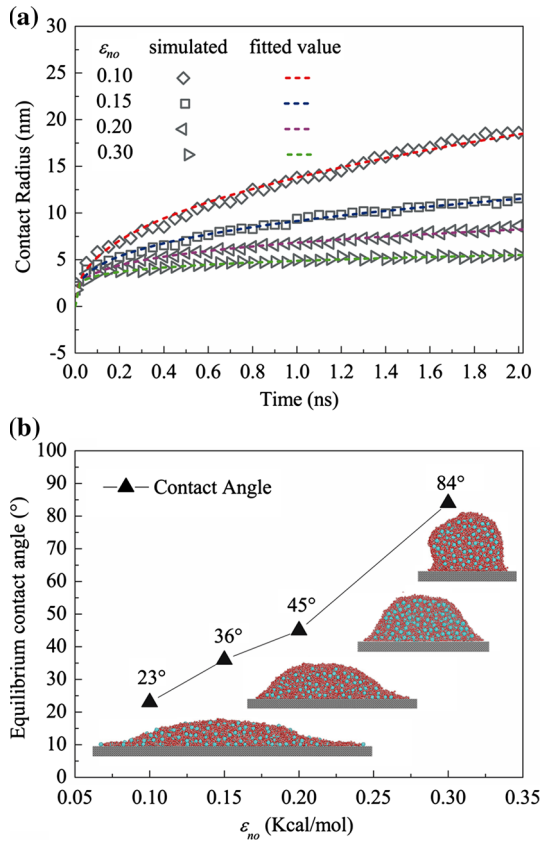

Fig. 4 Spreading results of nanofluid droplets containing nanoparticles with different surface properties ($\varphi = 5$ %). **a** The contact radius R as a function of spreading time t also shows a power exponential relationship: $R(t) = at^{1/n}$. **b** Comparison of the final MD snapshots and equilibrium contact angles for different models

Table 3 Fitting function parameters for different nanoparticle surface wettability models

Model number	φ (%)	ε_{no} (kcal/mol)	Fitting coefficient a	Fitting coefficient n
5	5	0.10	13.80	2.40
6	5	0.15	9.15	3.01
4	5	0.20	6.82	3.67
7	5	0.30	4.87	5.82

Then we note that when the nanoparticle volume fraction is small or the interaction between nanoparticles and liquid is small, the nanoparticles' effect is week. In model 5, even the nanoparticle volume fraction is large, but the nanofluid droplet displays similar spreading phenomenon as the water droplet and some of the nanoparticles escape from the droplet, both due to the week interaction $\varepsilon_{no} = 0.10$ kcal/mol. The presence of precursor film indicates that, during the spreading process of nanofluid droplet containing fewer nanoparticles and week hydrophilic nanoparticles, disjoining pressure plays an important role.

Besides, simulation of nanofluid droplets contain larger nanoparticles ($d \approx 1.0$ nm) with different surface wettability was performed as well. And a similar trend that increasing nanoparticle surface wettability results in inhibition in nanofluid droplet spreading was obtained.

The scaling law: $R(t) = at^{1/n}$ is widely used to describe the dynamic spreading of droplet (de Gennes 1985; Yuan and Zhao 2012, 2013a, b). The value of n reflects the dominate forces that drive the droplet spreading corresponding to different length scales and dimensionalities (Bonn et al. 2009). In terms of Tables 2 and 3, in our results, n varies within the range from 2 to 7, which identifies with the theoretical values in terms of two-dimensional droplet (Joanny and de Gennes 1986; Ren et al. 2010; Xu et al. 2004; Huppert 1982; Mchale et al. 1995). a is a coefficient relating to viscosity, surface

tension, etc. That is to say, nanoparticles change some bulk properties of the nanofluid droplet, such as nanofluid viscosity and thus give rise to different spreading mechanisms. From the analysis above, in the spreading of nanoparticles, surface tension, disjoining pressure and nanofluid viscosity are significance during nanofluid spreading. Then a competitive mechanism between surface tension, viscous force and disjoining pressure is proposed according to our present study.

4 Theoretical analysis of the droplet spreading based on the scaling law

4.1 A competitive mechanism between different forces

A theoretical analysis on the spreading mechanism considering the presence of nanoparticles has been done. The dominant forces in spreading process are discussed according to the values of n. The theoretical scaling law of droplet spreading is derived based on lubrication approximation theory for liquid film. Under non-slip condition, evolution equation of the two-dimensional liquid film is expressed as Eq. (4) (Oron et al. 1997; Zhao 2012).

$$\mu\frac{\partial h}{\partial t}-\frac{\partial}{\partial x}\left[\frac{1}{3}h^3\frac{\partial}{\partial x}\left(\phi\Big|_{z=h}-\gamma_{\mathrm{lv}}\frac{\partial^2 h}{\partial x^2}\right)\right]=0 \tag{4}$$

$$\int_0^{R(t)} h(x,t)\mathrm{d}x=\frac{1}{2}\Omega \tag{5}$$

where h is the film thickness and x and z indicate the horizontal and vertical directions, respectively. μ is the fluid viscosity, γ_{lv} is the interface tension between liquid and vapor phase. ϕ represents body force potential, including gravity, disjoining pressure, etc. It should be noted that gravity is ignored since the characteristic scale of our simulation system is much less than the capillary length (Bonn et al. 2009). Disjoining pressure is composed of van der Waals, electrostatic, steric and structural forces. In case of only van der Waals force is considered, disjoining pressure $\Pi(h)=-\frac{A}{6\pi h^3}$, in which A is Hamaker constant (Oron et al. 1997). Equation (5) is the reduced form of the continuity equation for incompressible fluid droplet.

1. First we consider an extreme condition that liquid droplet wets the substrate completely with an equilibrium angle $\theta_{\mathrm{eq}}=0^\circ$ and the final liquid film only contains several atom layers. The droplet spreading is mainly dominated by viscous force and disjoining pressure. Surface tension is rather small compared with the disjoining pressure. Thus, in Eq. (4), the term related to γ_{lv} is neglected. To our knowledge, $D(h)=-A/6\mu\pi h$ is defined as the spreading coefficient of the precursor film (Heine et al. 2005), so in Eq. (4) $\phi=D(h)=-A/6\mu\pi h$. Thus, Eq. (6) is derived from Eq. (4). Several studies have deduced that the dynamic spreading of precursor film follows $R\sim D(h)t^{1/2}$ (Heine et al. 2005; Ren et al. 2010; Xu et al. 2004),

$$\mu\frac{\partial h}{\partial t}+D\frac{\partial}{\partial x}\left(\frac{1}{h}\frac{\partial h}{\partial x}\right)=0 \tag{6}$$

Together with the continuity equations of incompressible fluid droplet Eq. (5), power law relationship between R and t, Eq. (7), is obtained.

$$R\sim D(h)t^{1/2} \tag{7}$$

2. If viscous force and surface tension dominate the droplet spreading process, Eq. (4) is reduced to Eq. (8). The spreading power law relationship in this case can be written in Eq. (9).

$$\mu\frac{\partial h}{\partial t}+\frac{1}{3}\gamma_{\mathrm{lv}}\frac{\partial}{\partial x}\left(h^3\frac{\partial^3 h}{\partial x^3}\right)=0. \tag{8}$$

$$R=\xi_R\left(\frac{\gamma_{\mathrm{lv}}\Omega^3}{24\mu}\right)^{1/7}t^{1/7}\sim t^{1/7}. \tag{9}$$

The scaling exponent n of droplet spreading for two-dimensional model should be within the range from 2 to 7. From the analyses above, we can conclude that spreading behaviors of water droplet and nanofluid droplets laden with nanoparticles are mainly affected by disjoining pressure $\Pi(h)$, viscous force f and surface tension γ_{lv}. The coefficient a and power exponent n reflect the competitive relationship of these forces in the dynamic spreading process.

It is obvious that the viscous force tends to hinder the droplet spreading, whereas the disjoining pressure promotes the spreading process by acting in the vicinity of the triple-phase contact line region. The presence of viscosity μ in both situations acts as an element to reduce the coefficient a, which means that the smaller a is, the lager the nanofluid viscosity will be.

For water droplet we studied, n is fitted to be 2.54. For nanofluid droplets with $\varphi=1$ % (model 2) and $\varphi=5$ % but containing low hydrophilic nanoparticles (model 5), the values of n are 2.86 and 2.40, respectively. All these values are very close to the 1/2 scaling law. But the value of a is 19.37 for model 2 and 13.8 for model 5, which are significantly smaller than that of water droplet, 22.54. This means that in both model 2 and model 5, the viscosity of nanofluid turns to be larger than water. Then it can be concluded that in these cases, disjoining pressure caused by the van der Waals force dominates the spreading behaviors.

Table 4 Composition of models for MSD calculation

Model number	φ (%)	ε_{no} (kcal/mol)	Number of water molecules N_w	Number of nanoparticles N_n
1′	0	0.20	7,199	0
2′	1	0.20	7,127	64
3′	3	0.20	6,983	193
4′	5	0.20	6,839	322
5′	5	0.10	6,839	322
6′	5	0.15	6,839	322
7′	5	0.30	6,839	322

The symbol ′ following the number indicates its origin corresponding model

In the discussion of nanoparticle volume fraction, the value of a decrease from 22.54 to 6.82 as φ varies from 0 to 5 %. That is to say, the larger φ is, the larger viscosity of nanofluid will be. As the nanoparticle volume fraction increases, n changes toward the 1/7 scaling law, which means that viscous effect becomes stronger and finally exceeds the disjoining pressure. But this does not mean that the disjoining pressure vanishes. As the nanoparticle volume fraction increases, the accumulation of nanoparticles cannot be neglected. The structural component of disjoining pressure and capillary force (Chengara et al. 2004; Weon and Je 2013) caused by nanoparticles in the vicinity of contact line is inferred to be influential.

In cases of models 4–7 with different nanoparticle surface wettabilities, the viscosity also shows a dramatically increase with the interaction between nanoparticles and water. When $\varepsilon_{no} = 0.30$ kcal/mol (model 7), n is 5.82, close to the 1/7 scaling law. This means that when the nanoparticles are hydrophilic enough, viscosity and surface tension dominate the nanofluid droplet spreading.

4.2 Quantitative analysis on viscosity of nanofluid

To support the competitive mechanism extracted from our simulation, viscosity of nanofluid in each model was calculated. Simulation system was a cubic box with side length of 6.2 nm, and periodic boundary conditions were applied in all directions. The water molecule number and nanoparticle number are nearly the same with each simulation case (models 1–7) discussed above, listed in Table 4. The interaction parameters are strictly the same with their corresponding models.

Mean-square displacements (MSD) of the nanofluids were calculated, and all cases show that the MSD is in linear relation with time t regardless of the nanoparticle concentration and interaction parameters, but with different slopes. Accounting for Eq. (10) (Du et al. 2007; Shu et al.

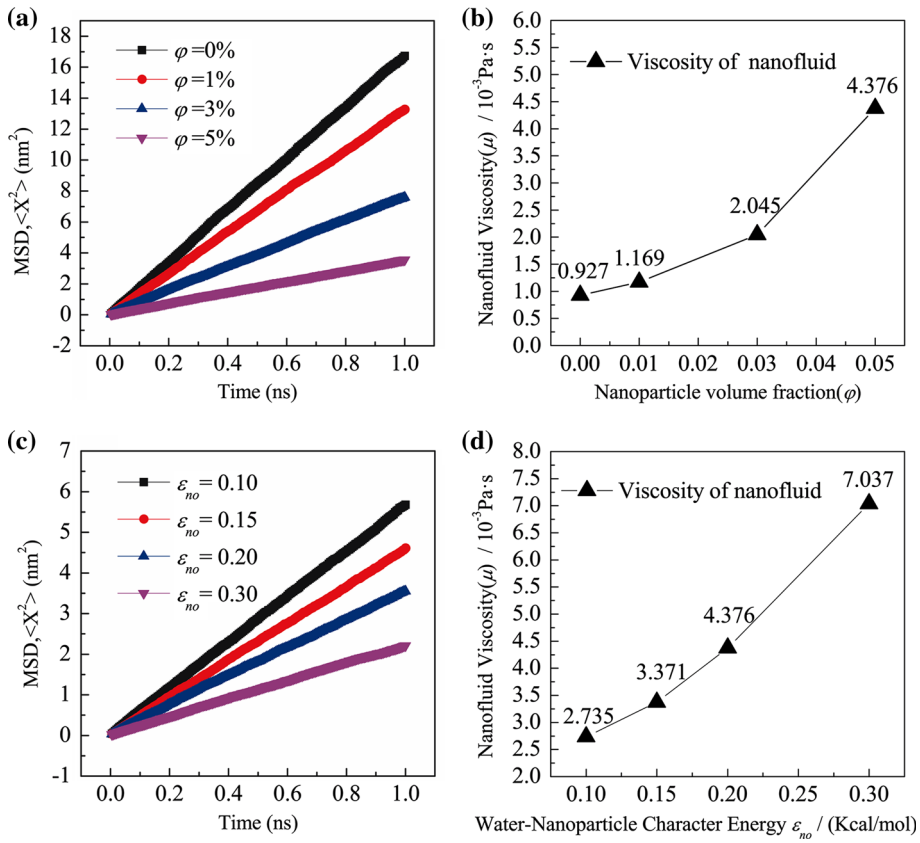

Fig. 5 Nanofluid viscosity of different models, calculated based on the MSD. **a**, **b** Nanofluid MSD and viscosity vary as the nanoparticle volume fraction increasing. **c**, **d** Nanoparticle–oxygen interaction energy effect on the MSD and viscosity of nanofluids with $\varphi = 5$ %

2013), the slope is 6 times of the self-diffusion coefficient D. Viscosity of nanofluid μ is derived by importing the Einstein relation Eq. (11) (Thomas and Mcgaughey 2008).

$$D = \frac{\langle x^2 \rangle}{6t}, \tag{10}$$

$$\mu = \frac{k_B T}{3\pi r_w} \frac{1}{D}, \tag{11}$$

where $\langle x^2 \rangle$ is the MSD of the nanofluids. k_B is the Boltzmann constant and r_w is the molecular diameter, which is set to be 0.17 nm (Thomas and Mcgaughey 2008). T is the simulation temperature, 298 K.

First we verified the calculated viscosity of water, 0.927×10^{-3} Pa s under 298 K. The experimental data under 298 K are about 0.890×10^{-3} Pa s (Coe and Godfery 1944; Kestin et al. 1978). The value is valid allowing for computational errors. As can be seen from Fig. 5, increasing the nanoparticle concentration and the interaction between nanoparticles and liquid would dramatically enhance viscosity of nanofluid. Specifically, viscosity of nanofluid is more than 7 times than that of water when $\varepsilon_{no} = 0.3$ kcal/mol ($\varphi = 5$ %). For the case of $\varepsilon_{no} = 0.5$ kcal/mol, the calculated viscosity of nanofluid exceeds 15 times of water. These results are evidences of the enhancement of internal cohesive of nanofluid when nanoparticle volume fraction or nanoparticle surface wettability increases. It turns out that results derived from this equation confirmed the analysis that as the nanoparticle volume fraction and wettability increase, nanofluid viscosity increased accordingly and thus results in changes in spreading dominate forces. Our simulation results are in good consistency with previous experiment studies (Timofeeva et al. 2009) that increasing nanoparticles volume fraction will increase the viscosity of nanofluid. Even at $\varphi = 5$ %, the viscosity is 3–5 times than that of base fluid. The variation of viscosity due to surface wettabilites of nanoparticles promotes the competitive position of the various forces acting on nanofluid droplets. This means that mediating viscosity of nanofluid plays an important role in the theory we proposed that the presence of nanoparticle tunes the spreading behavior of nanofluid droplet.

5 Conclusions

Understanding the wetting behavior of nanofluids on solid substrate is crucial for diverse applications. We have performed MD simulations to investigate spreading behaviors of water-based nanofluid droplets. By varying the nanoparticle volume fraction and their surface wettability, the nanoparticle-tuned spreading behavior of nanofluid droplet on solid substrate was studied. Theoretical analysis based on the lubrication approximation was conducted for the contact radius R as a function of spreading time t. We found that varying nanoparticle volume fraction and surface wettability will effectively regulate the spreading behaviors of nanofluid droplet. The dynamic spreading can be slowed down by increasing nanoparticle volume fraction, as well as by increasing nanoparticle surface wettability. Further analysis shows that increasing in nanoparticles concentration or wettability properties will dramatically increase the viscosity of nanofluid. A competitive mechanism of dominated forces during spreading process has been proposed, which indicates that the viscous force plays an important role. For nanofluid droplet laden with small nanoparticle volume fraction and that with high volume fraction but very low wettability nanoparticles, the disjoining pressure and viscous force dominate the spreading. However, the effect of viscous force is weaker than that of disjoining pressure. As the nanoparticle concentration increases, the effect of viscous force turns to be stronger. The nanofluid droplet spreading behavior gradually inclines to surface tension and viscous force dominated. When the nanoparticle concentration and surface wettability are high enough, viscous force dominates the nanofluid droplet spreading and other force influences turn to be weak. This work provides a foundation on which the spreading of nanofluid droplet can be understood from atomistic scale.

Acknowledgments This work was jointly supported by National Natural Science Foundation of China, Anhui Provincial Natural Science Foundation and the Fundamental Research Funds for the Central Universities of China.

References

Adao MH, De Ruijter M, Voue M et al (1999) Droplet spreading on heterogeneous substrates using molecular dynamics. Phys Rev E 59:746–750

Alava MJ, Dube M (2012) Droplet spreading and pinning on heterogeneous substrates. Phys Rev E 86:011607

Baby TT, Ramaprabhua S (2010) Investigation of thermal and electrical conductivity of graphene based nanofluids. J Appl Phys 108:124308

Berendsen HJC, Grigera JR, Straatsma TP (1987) The missing term in effective pair potentials. J Phys Chem 91:6269–6271

Bonn D, Eggers J, Indekeu J et al (2009) Wetting and spreading. Rev Mod Phys 81:739–805

Chen HG, Bodmeier R (1990) Indomethacin polymeric nanosuspensions prepared by microfujidization. J Control Release 12:223–233

Chengara A, Nikolov AD, Wasan DT et al (2004) Spreading of nanofluids driven by the structural disjoining pressure gradient. J Colloid Interface Sci 280:192–201

Choi SUS, Eastman JA (1995) Enhancing thermal conductivity of fluids with nanoparticles. In: Siginer DA, Wang HP (eds) Developments and applications of non-Newtonian flows. American Society of Mechanical Engineers, New York, pp 99–105

Chon CH, Kihm KD, Lee SP et al (2005) Empirical correlation finding the role of temperature and particle size for nanofluid (Al_2O_3) thermal conductivity enhancement. Appl Phys Lett 87:153107

Coe JR, Godfery TB (1944) Viscosity of water. J Appl Phys 15:625

de Gennes PG (1985) Wetting—statics and dynamics. Rev Mod Phys 57:827–863

De Ruijter MJ, De Coninck J, Oshanin G (1999) Droplet spreading: partial wetting regime revisited. Langmuir 15:2209–2216

Du XS, Li QX, Chen Y et al (2007) Pair-hopping characteristic of lithium diffusive motion in li-doped beta-phase manganese phthalocyanine. J Phys Chem B 111:10064–10068

Ganguly S, Sikdar S, Basu S (2009) Experimental investigation of the effective electrical conductivity of aluminum oxide nanofluids. Powder Technol 196:326–330

Han J, Kim C (2012) Spreading of a suspension drop on a horizontal surface. Langmuir 28:2680–2689

Harkins WD, Feldman A (1922) Films the spreading of liquids and the spreading coefficient. J Am Chem Soc 44:2665–2685

Heine DR, Grest GS, Webb EB (2005) Surface wetting of liquid nanodroplets: droplet-size effects. Phys Rev Lett 95:107801

Hong TK, Yang HS, Choi CJ (2005) Study of the enhanced thermal conductivity of Fe nanofluids. J Appl Phys 97:064311

Huppert HE (1982) The propagation of two-dimensional and axisymmetric viscous gravity currents over a rigid horizontal surface. J Fluid Mech 121:43–58

Joanny JF, de Gennes PG (1986) Upward creep of a wetting fluid—a scaling analysis. J Phys 47:121–127

Kestin J, Sokolov M, Wakeham WA (1978) Viscosity of liquid water in range −8 C to 150 C. J Phys Chem 7:941–948

Kole M, Dey TK (2010) Thermal conductivity and viscosity of Al2O3 nanofluid based on car engine coolant. J Phys D Appl Phys 43:315501

Kondiparty K, Nikolov A, Wu S et al (2011) Wetting and spreading of nanofluids on solid surfaces driven by the structural disjoining pressure: statics analysis and experiments. Langmuir 27: 3324–3335

Lee S, Choi SUS, Li S et al (1999) Measuring thermal conductivity of fluids containing oxide nanoparticles. J Heat Trans 121:280–289

Lin JQ, Zhang HW, Chen Z et al (2011) Simulation study of aggregations of monolayer-protected gold nanoparticles in solvents. J Phys Chem C 115:18991–18998

Liu GL, Kim J, Lu Y et al (2006) Optofluidic control using photothermal nanoparticles. Nat Mater 5:27–32

Mchale G, Newton MI, Rowan SM et al (1995) The spreading of small viscous stripes of oil. J Phys D Appl Phys 28:1925–1929

Minea AA, Luciu RS (2012) Investigations on electrical conductivity of stabilized water based Al2O3 nanofluids. Microfluid Nanofluid 13:977–985

Nieminen JA, Abraham DB, Karttunen M et al (1992) Molecular-dynamics of a microscopic droplet on solid-surface. Phys Rev Lett 69:124–127

Oppenheim RC (1981) Solid colloidal drug delivery systems: nanoparticles. Int J Pharm 8:217–234

Oron A, Davis SH, Bankoff SG (1997) Long-scale evolution of thin liquid films. Rev Mod Phys 69:931–980

Pilkington GA, Briscoe WH (2012) Nanofluids mediating surface forces. Adv Colloid Interface 179:68–84

Plimpton SJ (1995) Fast parallel algorithms for short-ranged molecular dynamics. J Comput Phys 117:1–19

Prasher R, Song D, Wang JL et al (2006) Measurements of nanofluid viscosity and its implications for thermal applications. Appl Phys Lett 89:133108

Ren WQ, Hu D, Weinan E (2010) Continuum models for the contact line problem. Phys Fluids 22:102103

Ritos K, Dongari N, Borg MK et al (2013) Dynamics of nanoscale droplets on moving surfaces. Langmuir 29:6936–6943

Shu XL, Tao P, Li XC et al (2013) Helium diffusion in tungsten: a molecular dynamics study. Nucl Instrum Methods Phys Res Sect B 303:84–86

Song FH, Li BQ, Liu C (2013) Molecular dynamics simulation of nanosized water droplet spreading in an electric field. Langmuir 29:4266–4274

Tanner LH (1979) Spreading of Silicone oil drops on horizontal surfaces. J Phys D Appl Phys 12:1473–1484

Thomas JA, Mcgaughey AJH (2008) Reassessing fast water transport through carbon nanotubes. Nano Lett 8:2788–2793

Timofeeva EV, Routbort JL, Singh D (2009) Particle shape effects on thermophysical properties of alumina nanofluids. J Appl Phys 106:014304

Trokhymchuk A, Henderson D, Nikolov A et al (2001) A simple calculation of structural and depletion forces for fluids/suspensions confined in a film. Langmuir 17:4940–4947

Vafaei S, Borca-Tasciuc T, Podowski MZ et al (2006) Effect of nanoparticles on sessile droplet contact angle. Nanotechnology 17:2523–2527

Wang FC, Wu HA (2013) Enhanced oil droplet detachment from solid surfaces in charged nanoparticle suspensions. Soft Matter 9:7974–7980

Wasan DT, Nikolov AD (1999) In supramolecular structure in confined geometries. In Marne G, Warr G (eds) ACS Symp Ser vol 736, pp 40–53

Wasan DT, Nikolov AD (2003) Spreading of nanofluids on solids. Nature 423:156–159

Weon BM, Je JH (2013) Self-pinning by colloids confined at a contact line. Phys Rev Lett 110:028303

Xu H, Shirvanyants D, Beers K et al (2004) Molecular motion in a spreading precursor film. Phys Rev Lett 93:206103

Yuan QZ, Zhao YP (2010) Precursor film in dynamic wetting, electrowetting, and electro-elasto-capillarity. Phys Rev Lett 104:246101

Yuan QZ, Zhao YP (2012) Topology-dominated dynamic wetting of the precursor chain in a hydrophilic interior corner. Proc R Soc Math Phys 468:310–322

Yuan QZ, Zhao YP (2013a) Multiscale dynamic wetting of a droplet on a lyophilic pillar-arrayed surface. J Fluid Mech 716:171–188

Yuan QZ, Zhao YP (2013b) Wetting on flexible hydrophilic pillar-arrays. Sci Rep 3:1944

Zhao YP (2012) Physical mechanics of surfaces and interfaces. Beijing, Science Press, pp 552–560